Laboratory experiments on mesoscale vortices colliding with multiple islands

Aya Tanabe
Imperial College London

July 18, 2006

1 Introduction

1.1 Oceanic background

Mesoscale vortices have recently been recognized to play an important role in redistribution and transport of water properties (e.g. temperature, salinity) around the oceans. The interaction of vortices with seamounts, submerged ridges, or islands might result in enhanced and localized transfer of anomalous fluid from the vortices to the surrounding environment. In addition, the interaction could end in the formation of new vortices downstream otherwise complete destruction of the incident vortices. This topic has been investigated for the past several decades for e.g. Meddies in the eastern North Atlantic, Agulhas rings in the eastern South Atlantic, and North Brazil Current (NBC) rings in the western tropical Atlantic. In the current study, we will focus on, in particular, the behaviour of the last kind of vortices, NBC rings which interact with the Lesser Antilles.

It is believed that NBC rings are one of the leading mechanisms for transporting the upper ocean equatorial and South Atlantic water into the North Atlantic as part of the Meridional Overturning Cell (MOC). The MOC transports cold deep water southward across the equator and, to be balanced, transports upper ocean South Atlantic waters northward. In the upper layers, the NBC is a northward flowing western boundary current that carries warm water across the equator along the coast of Brazil (Figure 1). Near $5^o - 10^o\, N$, the NBC separates sharply from the coastline and retroflects to feed the eastward North Equatorial Counter Current (NECC) [7]. During its retroflection, the NBC occasionally pinches off isolated anticyclonic warm-core vortices exceeding $450\, km$ in overall diameter,

$2\,km$ in vertical extent, and swirling at speed approaching $100\,cms^{-1}$. These NBC rings move north-westward toward the Caribbean at $8-17\,cms^{-1}$ on a path parallel to the coastline of Brazil. As part of the MOC, in most cases, they then interact with a complex island chain, the Antilles islands [6] and enter the Caribbean Sea. (Episodically, they enter the North Atlantic subtropical gyre.) The inflow into the Caribbean Sea ultimately feeds the Florida Current which is now recognized to be a fundamental passage for northward transport of upper ocean waters in the global thermohaline circulation. Therefore, the Atlantic MOC (hence NBC rings) is an important element of the global thermohaline circulation and a fundamental component of the global climate system. Recent observations reveal that relatively large (average diameter $200\,km$) energetic anticyclonic vortices were found downstream of the Antilles islands in the Eastern Caribbean Sea and translated westward in the central part of it whereas cyclonic vortices were observed primarily near boundaries in the Eastern Caribbean Sea [11] (Figure 2). Unfortunately, it is difficult, by observations, to know whether or not such large anticyclonic and cyclonic vortices observed in the Eastern Caribbean Sea have been produced as a consequence of the interaction between NBC rings and the Antilles islands, and if so, how they have been formed. In the present work, we shall try to answer part of this question through laboratory experiments.

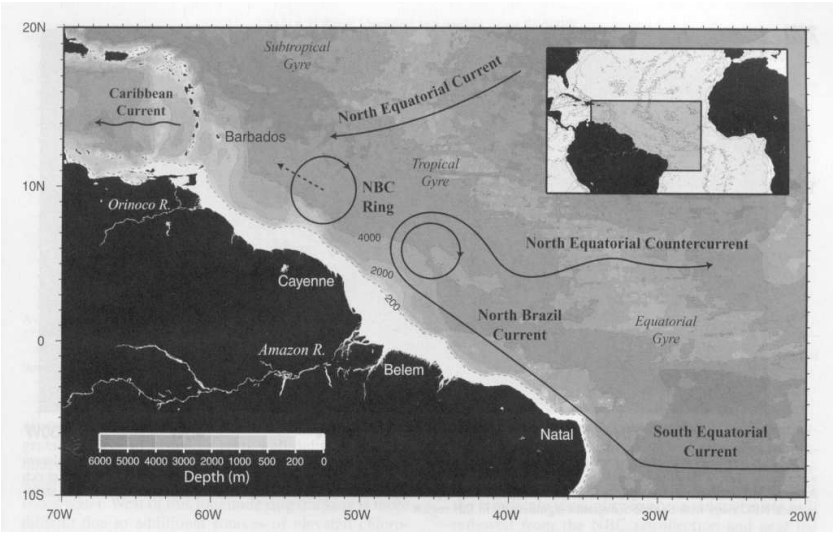

Figure 1: Sketch of the upper-ocean circulation in the western tropical Atlantic from [5].

1.2 The previous works

Before mentioning a possible mechanism for the large anticyclonic and cyclonic vortices formation in the Eastern Caribbean Sea, let us introduce briefly two previous works on

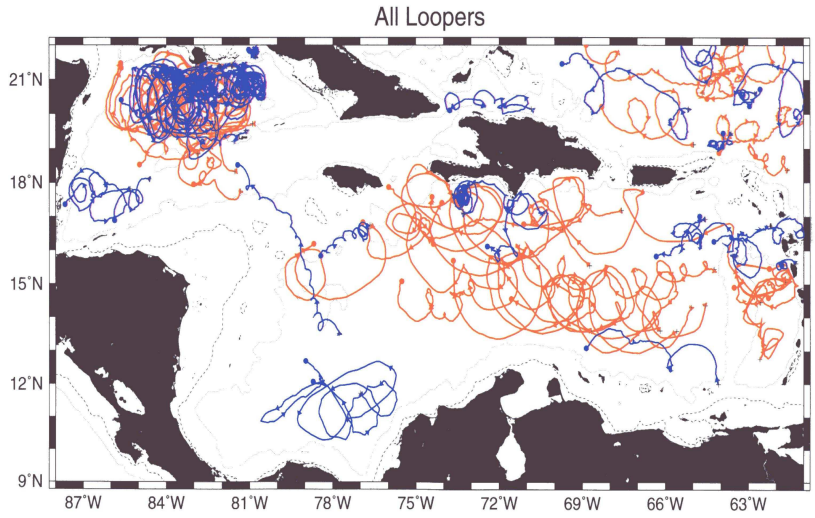

Figure 2: Drift trajectories of 28 cyclones (blue) and 29 anticyclones (red). Anticyclones seem to be dominant in the Eastern Caribbean Sea between 65^0W and 75^0W, from [11].

interaction of vortices with multiple islands.

The interaction of a monopolar, self-propagating cyclonic vortex with two circular cylinders was investigated in the laboratory [2] (Figure 3 (a)). Typically after the vortex came in contact with the two cylinders, the outer edge of the vortex was peeled off and a so-called "streamer" (or two "streamers") went around one of the cylinders (or each of the cylinders) (Figure 3 (b)). When the streamer velocity v_s was large enough (i.e. $400 < Re < 1100$ where $Re = v_s d/\nu$, and d is the diameter of the incident vortex), the "streamer(s)" turned into a new cyclonic vortex (or two new vortices). During the experiments in [2], three parameters were varied: G, the separation between the cylinders; d; and Y, the perpendicular distance of the center of the vortex from an axis passing through the center of the gap between the cylinders (see Figure 3 (a)). One of the remarkable observations in [2] is that the flow within the vortex was "funneled" between the two cylinders and formed a dipole vortex, much like water ejected from a circular nozzle generates a dipole ring. This behaviour occurred provided that $-2 < Y/g < 0$, $0.25 \leq G/d \leq 0.4$, and $Re_G > 200$, where $g = G/2$, $Re_G = U_G G/\nu$ is the Reynolds number based on a length scale $\sim O(G)$, and U_G is the maximum velocity of the vortex fluid in the gap. The size of the created cyclonic and anticyclonic vortices (i.e. a dipole) was smaller than that of the original vortex.

A second relevant work is a numerical investigation of the interaction of both a self-propagating and an advected vortex with multiple islands [13]. The islands were represented by thin vertical walls aligned in the North-South direction with gaps having a width of 20 % of the vortex diameter. This study showed that if the individual islands were small

compared with the vortex radius (e.g. $L/R_i = 0.3$ where L is the island length, R_i is the initial vortex diameter[1]), the vortex reorganized in the basin downstream of the islands, whereas it always split into multiple offsprings if the islands were large (e.g. $L/R_i = 1.5$) (Figure 4). Moreover, intense vortices experienced relatively greater amplitude loss than weak vortices. The results of [13] may give an account of the observations of anticyclones in the Eastern Caribbean Sea, but the generation of cyclones in the Sea can not be explained by their results as no cyclones were seen in [13].

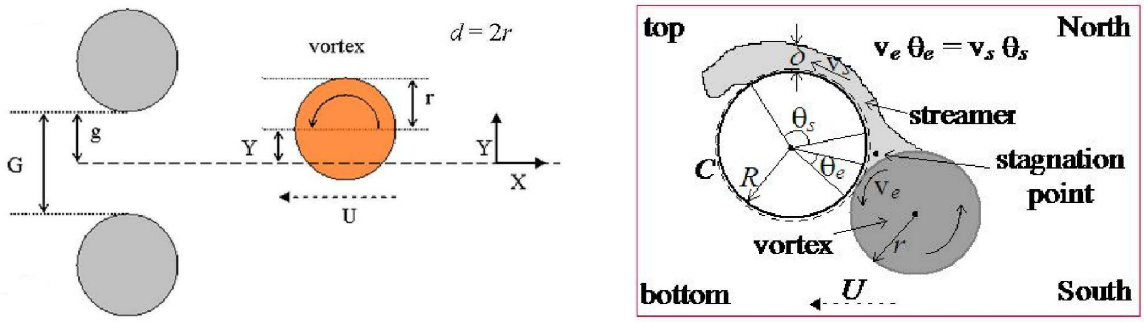

(a) (b)

Figure 3: (a): sketch illustrating the geometry of the encounter between the vortex and two cylinders, from [2]. The diameter of the cylinders, D, is $5\,cm$. (b): sketch of a streamer, from [3].

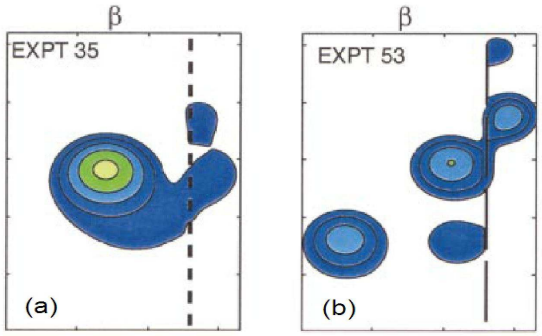

Figure 4: Multiple-islands numerical experiments from [13]. (a): $L/R_i = 0.3$. (b): $L/R_i = 1.5$.

1.3 Hypothesis

Since the Lesser Antilles have passage width between $30 - 60\,km$ and the approaching NBC vortices' size varies between $200 - 400\,km$, G/d lies in the range $0.07 - 0.3$. Although this

[1]The definition of the vortex initial radius is not stated in [13], hence R_i and d (defined in [2]) are not necessarily equal.

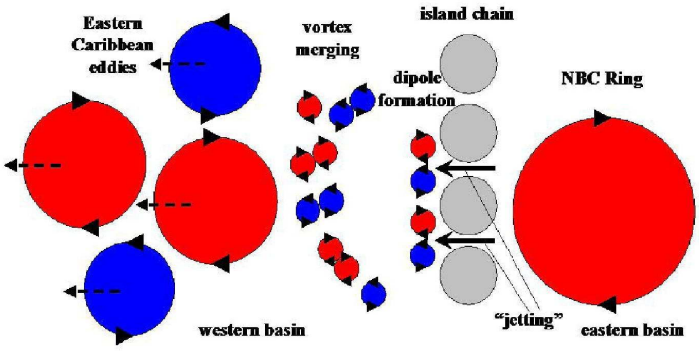

Figure 5: Sketch illustrating a possible formation mechanism for the large Eastern Caribbean vortices [11].

range does not exactly fit in $0.25 \leq G/d \leq 0.4$ obtained in [2], it is natural to anticipate that dipole formation is likely to occur downstream of the Lesser Antilles' passages. Assuming that several pairs of dipoles are formed at western side of the islands, we expect that transition from small scale vortices to large scale structures will occur by the merging of vortices of like sign (Figure 5). When rotation is present, the scale to which the vortices grow is determined by instability processes that inhibit vortices to grow to scales larger than the Rossby radius of deformation [9]. The coalescence of same sign vortices is similar to the well-known feature of inverse energy cascade in two-dimensional flow [10]. Finally, vortices having a diameter of the order of the Rossby radius of deformation will form and drift westward due to the planetary β-plane (Figure 5).

2 The experiments

2.1 Experimental apparatus

The experiments were performed in a square tank of depth $45\,cm$, length and width of $115\,cm$. Both 'top-view' and 'side-view' illustrations of the apparatus are shown in Figures 6 & 7. Some experiments were carried out in a much smaller tank (depth $36\,cm$, length and width $60\,cm$). However, as we are interested in knowing not only whether or not *several* dipoles are formed when vortices interact with a chain of obstacles, but also the fate of the dipoles (if they are really formed), it was appropriate to focus on experiments performed in the larger tank. The apparatus in Figures 6 & 7 was mounted concentrically on a $2\,m$-diameter rotating turntable with a vertical axis of rotation. The sense of rotation of the turntable was anticlockwise. A square tank was used to avoid optical distortion from side views associated with a circular tank. The tank had a sloping bottom which makes an angle α to the bottom of the tank in order for a vortex to self-propagate leftward when looking

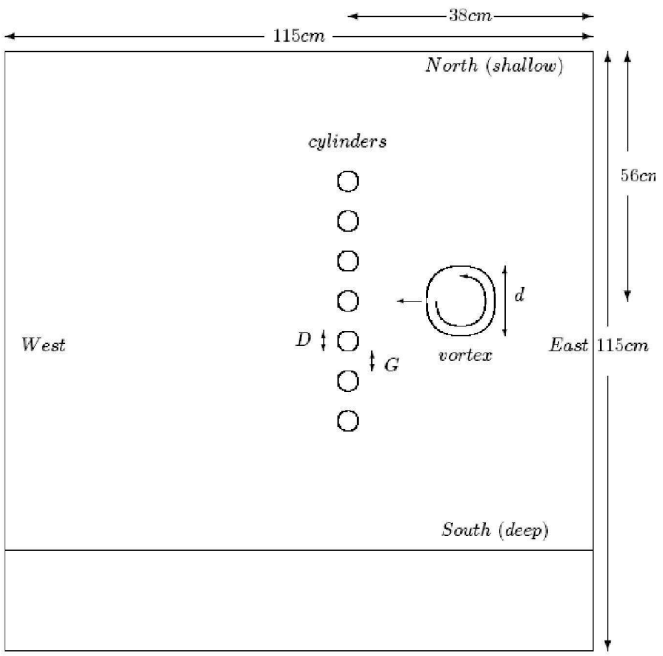

Figure 6: Sketch of the experimental apparatus: top view.

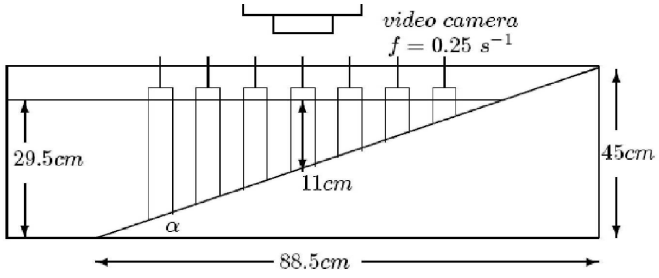

Figure 7: Sketch of the experimental apparatus: side view.

upslope [4]. We note that there is an analogy between the β-plane effect and the sloping topography effect provided that the angle of the slope α and the Rossby number Ro (the ratio of the advection term to the Coriolis term in the horizontal momentum equations) are sufficiently small [4]. The shallowest part of the tank corresponds to North. Hence, East is to the right when looking upslope, West is to the left, and South is the deepest part of the tank. The tank was filled with fresh water, which was initially in solid body rotation. Seven circular cylinders whose diameter is D were aligned in the North-South direction, and each of them was separated by a gap G as shown in Figures 6. The position of the central cylinder (the fourth one from North (or South)) was always fixed. However, the position of the other cylinders could be changed to vary the value G. The depth of the water at the

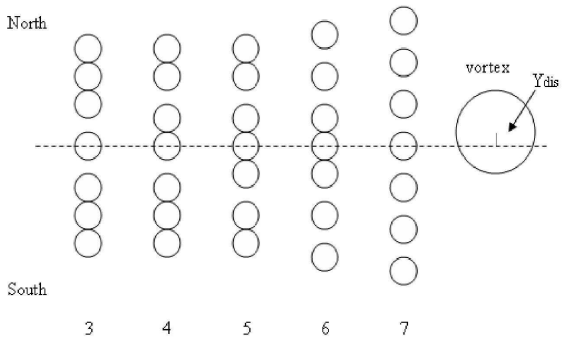

Figure 8: The five configurations of the obstacles used in the experiments. The position of the fourth cylinder from North (or South) was kept fixed.

central cylinder, h_0, was chosen to be $11\,cm$ which was much larger than the Ekman layer depth $\delta_{Ek} = \sqrt{2\nu/f} \approx 3\,mm$, where ν is the kinematic viscosity of the water and f is the Coriolis parameter. The bottom of each cylinder was sliced at an angle so it rested flush with the sloping bottom.

A barotropic cyclonic vortex was generated by placing an ice cube in the water [14], a method dynamically similar to withdrawing fluid from a sink positioned on the sloping bottom. The water surrounding the ice cube, due to conduction, becomes colder than the surrounding water and sinks as a cold plume, forming a cold dense lens within the thin bottom Ekman layer. The dense plume induces inward velocities along the entire column depth above the bottom lens, and then, influenced by the Coriolis force, the water column (above the dense lens) starts to spin cyclonically. In order to conserve mass, the dense fluid in the bottom Ekman layer flows radially outwards with a rapid velocity in comparison to the rotation period of the tank and thus a dense anticyclonic vortex does not form on the bottom. The fluid within the dense lens moves downslope together with the established barotropic vortex above it. Influenced by the Coriolis force, both the cyclonic water column and the cold lens change their direction and start drifting westward with a very small meridional displacement. Although NBC rings are anticyclonic vortices, in the laboratory it was not possible to reproduce stable barotropic anticyclones as they tend to be centrifugally unstable [8] and become non-axisymmetric in a few rotation periods. Furthermore, NBC rings have a baroclinic structure and move within a stratified fluid. As shown by [3], the use of cyclonic vortices does not limit the generality of the results, which can be easily extended to anticyclones. In particular, the circulation equation around the obstacle and the equation relating the streamer velocity to the vortex velocity (the equation in Figure 3 (b)) still hold for anticyclones. We neglected the effect of a stratified environment and

the influence of the advection mechanism on the interaction in our present study. Lack of stratification is possibly the weakest point of our model but the good agreement between the results obtained in [1, 2, 3] and the oceanic observations suggests that stratification does not invalidate the relevance of the results discussed here.

For all the experiments, the Coriolis parameter f was fixed at 0.25 s^{-1}, and $\nu = 0.01\,cm^2 s^{-1}$. The bottom slope was set at $s = \tan\alpha = 0.5$, where α is the angle between the sloping bottom and the horizontal so that the self-propagating vortex could move westward with a speed $U \approx 0.2\,cms^{-1}$. The vortex was produced approximately $20\,cm$ westward of the eastern wall of the tank. Hence, the vortex moved $20\,cm$ westward and interacted with the chain of cylinders before the spindown time $\tau = h_0/\sqrt{\nu f} \approx 200\,s$. The diameter of the cylinders, D, is $3.3\,cm$. Three values for the size of the gaps, $G = 3,\ 1.5,\ 0.7\,cm$ and five types of configurations of the obstacles (Figure 8) were studied. The azimuthal velocity profile of the vortex in the experiments, v_θ, is similar to that of a Rankine vortex with an approximately constant vorticity (solid body rotation) for $0 \leq r' \leq r'_{max}$ and a velocity which decays roughly like $1/r'$ for $r' > r'_{max}$, where r' is the radial coordinate originating in the vortex center. We define the vortex radius r to be not r'_{max} where the azimuthal velocity of the vortex is maximum, but the radial distance (from the center of the vortex) where the velocity has decayed by approximately 30 % (i.e. $r = r'_{max}/0.7$). This definition for the vortex radius is same as the one in [1, 2]. The *incident* vortex diameter d ranged between $7.6 - 19\,cm$ due to non-uniformity of the size of the ice cubes used.

2.2 Measurements

A video camera was mounted above the tank and was fixed to the turntable so that we were able to observe the flow in the rotating frame. For half of the experiments, the vortex was made visible by using a white sloping bottom, dripping dye (food coloring) on the ice cube and adding buoyant paper pellets on the free surface. The motion of the dyed vortex was also observed from the side of the tank. For the rest of the experiments, the paper pellets on the free surface and a black sloping bottom were used in order to measure the velocity field and to calculate, for instance, the circulation of the vortex. Images were grabbed from the recorded video tape by using XCAP. The time interval between each image was $0.15\,s$. An image processing software, DigiFlow was used to do particle tracking, and then calculate the velocity field by mapping the individual velocity vectors onto a rectangular grid using a spatial average over $2\,cm$ and the time average over $10\,s$. Once the gridded velocity was obtained, quantities such as the position (center), the radial distance r' where the velocity is maximum (i.e. r'_{max}), and the circulation of the vortex (before and after the interaction with the obstacles) were computed by using Matlab. Let x, y be the zonal and meridional

coordinates in Figure 9, respectively. Further, let us define U, V to be the x-, y-component of the vortex velocity, respectively. The position of the vortex center was determined as the intersection of two lines; one is a line where $|U|$ is maximum and parallel to the y-axis while the other is a line where $|V|$ is maximum and parallel to the x-axis (red lines in Figure 9). Two different r'_{max} were computed by defining two radial distances from the vortex center, namely

$$r_{max} = max(r_1,\, r_2,\, r_3,\, r_4)\ , \qquad r_{av} = average(r_1,\, r_2,\, r_3,\, r_4)\ ,$$

where r_1 is the radial distance from the vortex center to the eastward location where $|V|$ is maximum, r_2 is the distance from the vortex center to the northward location where $|U|$ is maximum, etc. Defining $r_{max},\ r_{av}$ was important particularly when the vortex was distorted. Since r_{av} turned out to be better in general (that is, $|U|$ and $|V|$ are almost maximum at $r' = r_{av}$), we focused only on the case $r'_{max} = r_{av}$. Once r'_{max} was obtained, the circulations of the vortex $\Gamma_B,\ \Gamma_A$ (before and after the interaction, respectively) were computed:

$$\Gamma_B = A \sum_i \omega_i\ ,$$

where A is the area of the single grid square, and ω_i is the relative vorticity at each grid point within $r' = r'_{max} = r_{av,\,B}$ ($r_{av,\,B} = r_{av}$ before the interaction). A similar expression can be written for Γ_A. By looking at the video tape, it is possible to know the number of the offsprings N, whether or not a dipole was formed (or several dipoles were formed), and whether there was a backward flow (fluid flowing between the cylinders from west to east) or not.

3 Experimental results

3.1 $G = 3\,cm$

Let us firstly discuss the results for $G = 3\,cm$ with $d = 7.6 \sim 19\,cm$ ($0.16 \leq G/d \leq 0.4$) because it corresponds to the kind of geometry found when the NBC rings interact with the Lesser Antilles. As soon as a vortex encountered the obstacles, a dipole almost always formed for all the configurations showed in Figure 8. However, the formation of two or more dipoles *never* occurred although the vortex extended for several cylinder and gap lengths. After a dipole formed, the cyclonic part of the dipole became dominant. Depending on the configurations of the obstacles and the initial vortex position, a relatively large cyclonic offspring was produced either directly from the cyclonic part of the dipole, or from the "remnant" of the original vortex at the gap positioned just "South" of the gap where the dipole was formed. (The vortex moved south due to its image vortex. The degree of

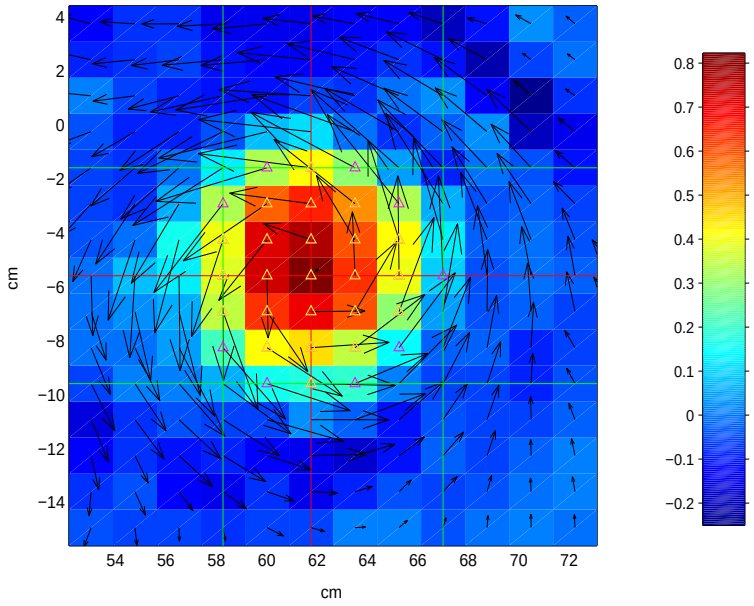

Figure 9: Velocity (arrows) and vorticity (colors) fields of a typical vortex in the experiments. The intersection of the red lines is the center of the vortex. r_i ($i = 1 \ldots 4$) are perpendicular distances from the center to the green lines. The circulation based on r_{av} is the sum of the vorticity at each of the yellow triangles.

the southward movement of the vortex depends on the configurations.) The number of offsprings, N, was 1 in most cases, rarely 2, and never 0. The formation of large vortices downstream of the obstacles is surprising as the gap width was only $16 \sim 40\,\%$ of the initial vortex diameter. Figures 10 & 11 show two laboratory experiments with G = 3 cm. Figure 10 shows the velocity and vorticity fields for a configuration 7, while Figure 11 shows an experiment with configuration 3 in which a white sloping bottom and dye were used to visualize the flow. By Figures 12 & 13, our experimental results and the numerical observations [13] discussed in §1.2 can be compared. According to Figure 12, the relative reduction of vortex intensity tends to be large (small Γ_A/Γ_B) for intense vortices (large Γ_B), as observed in [13]. Figure 13(a) (Figure 13 (b)) is a plot of '$D_{isl}/r_{av,\,B}$ vs N' ('$D_{isl}/r_{av,\,B}$ vs Backward flow'), where D_{isl} is the total length of the 'middle' island (e.g. $D_{isl} = D = 3.3\,cm$ for configuration 3, $D_{isl} = 2D = 6.6\,cm$ for configuration 4 etc). So $D_{isl}/r_{av,\,B}$ is equivalent to L/R_i used in [13]. Figure 13 (a) shows that, in most cases, $N = 1$, independently of the value of $D_{isl}/r_{av,\,B}$ (or L/R_i). This result is in disagreement with the main result of [13]. On the contrary, Figure 13 (b) agrees with a result of [13] because there is a backward flow when $D_{isl}/r_{av,\,B}$ (or L/R_i) is small. ([13] says a vortex did not 'notice' the existence of the islands if L/R_i is small.)

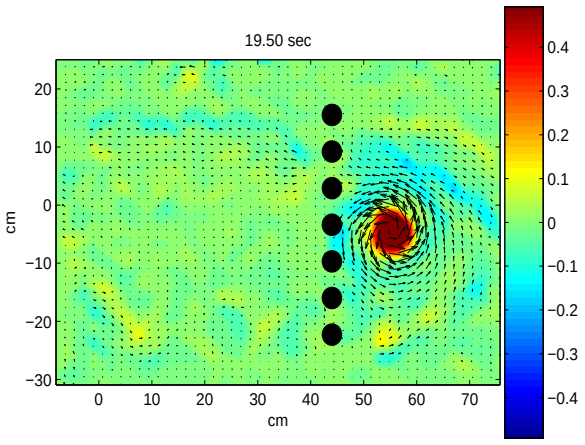

(a)

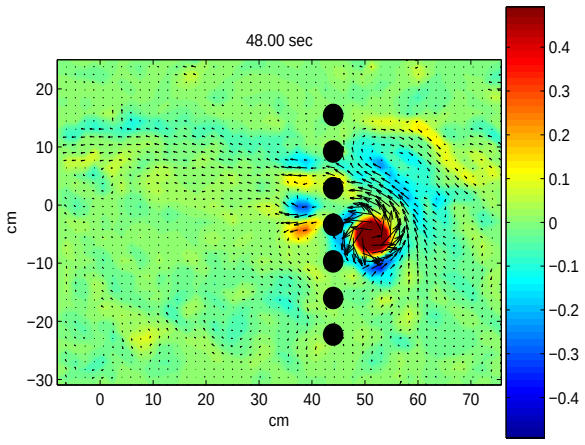

(b)

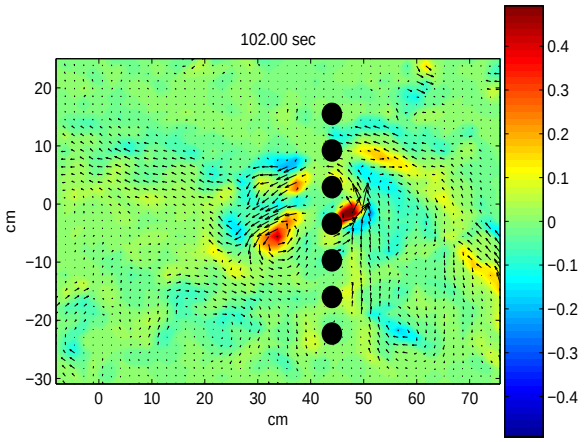

(c)

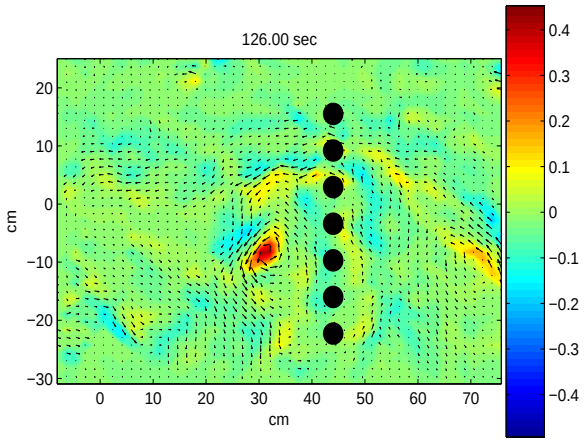

(d)

Figure 10: Velocity and vorticity fields for a configuration 7 experiment: (a) just before the interaction, $t = 19.5\,s$; (b) dipole formation, $t = 48\,s$; (c) the cyclonic part became dominant, $t = 102\,s$; (d) offspring formation, $t = 126\,s$.

3.2 $G = 1.5\,cm,\ 0.7\,cm$

When G was decreased, a different behaviour was observed: when $G = 1.5\,cm$, a small dipole still formed and the cyclonic part was dominant, and $N = 0$ or 1. When $G = 0.7\,cm$, a small portion of the vortex leaked through the gaps but no coherent structure was formed (i.e. always $N = 0$). The reason why the vortex generation was suppressed for $G = 0.7\,cm$

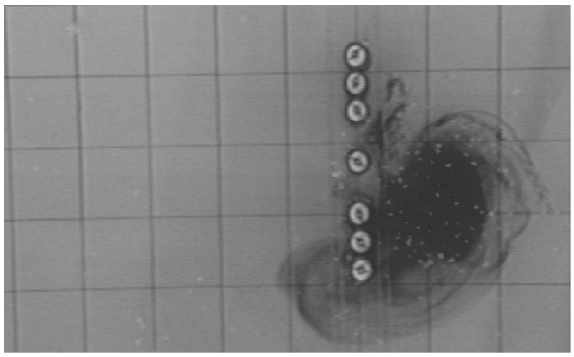

(a): $t = 7\,s$

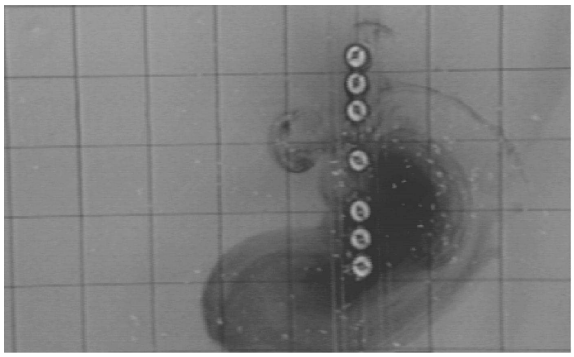

(b): $t = 48\,s$

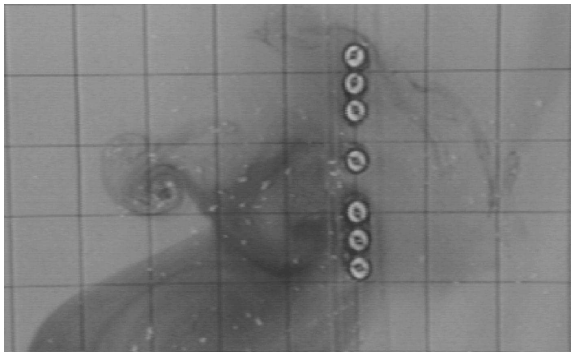

(c): $t = 144\,s$

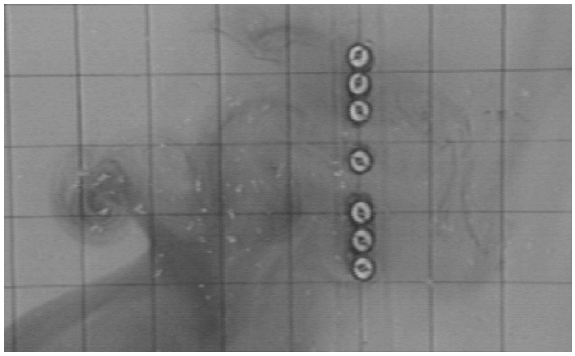

(d): $t = 182\,s$

Figure 11: A dye experiment for a configuration 3: (a) just before the interaction, $t = 7\,s$; (b) dipole formation, $t = 48\,s$; (c) the cyclonic part became dominant, $t = 144\,s$; (d) offspring formation, $t = 182\,s$.

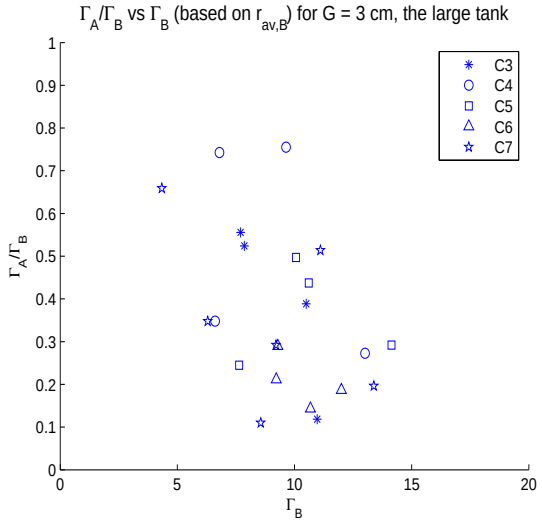

Figure 12: Γ_A/Γ_B vs Γ_B. The legend represents the configurations of the obstacles illustrated in Figure 8.

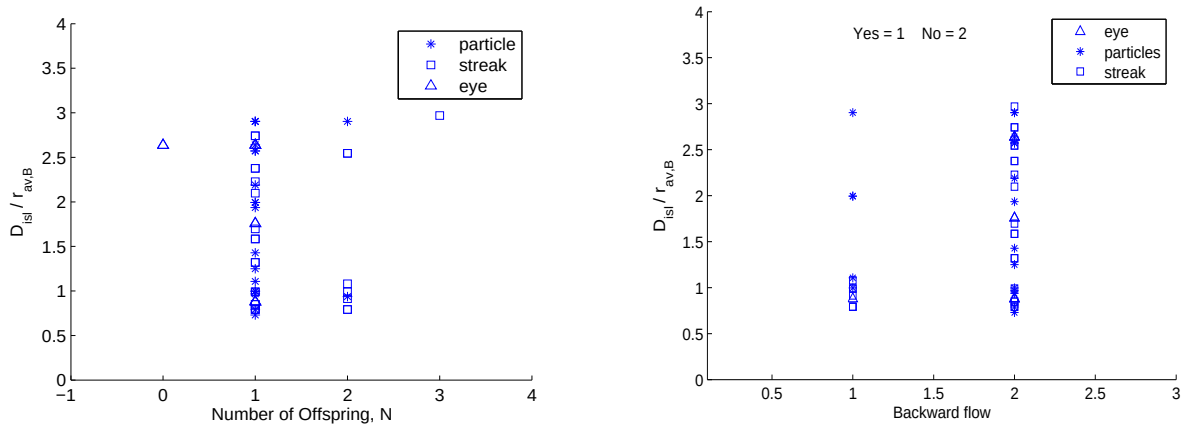

(a) (b)

Figure 13: (a): $D_{isl}/r_{av,\,B}$ vs N where D_{isl} is the total length of the 'middle' island (see the text for details), and $r_{av,\,B}$ is r_{av} before interaction with the cylinders. (b): $D_{isl}/r_{av,\,B}$ vs 'Backward flow'. $*$ are experiments with a black bottom slope, analysed by particle tracking. $\square$ and $\triangle$ are experiments with a white bottom slope and dye, analysed by streak and eyes, respectively.

and was reduced for $G = 1.5\,cm$ might be explained by considering the thickness of the boundary layers (b.ls) over the vertical walls of the obstacles. (We are interested in only the zonal b.ls since the flow through the gaps is zonal.) On the f-plane, the b.l thickness δ is expressed as

$$\delta = L E_H^{\frac{1}{2}} / E_L^{\frac{1}{4}} = \nu^{\frac{1}{4}} H^{\frac{1}{2}} / \Omega^{\frac{1}{4}} \ ,$$

where $E_L = \nu/(\Omega L^2)$ is the Ekman number based on the horizontal length scale L, $E_H = \nu/(\Omega H^2)$ is the Ekman number based on the vertical length scale H, and Ω is the rotation rate of the system. In the laboratory, $\nu = 0.01\,cm^2 s^{-1}$, $\Omega = f/2 = 0.125\,s^{-1}$, $L = D = 3.3\,cm$, and $H = h_0 \approx 10\,cm$.

$$\Longrightarrow \boxed{\delta = 1.68\,cm} \ .$$

On the β-plane, two kinds of zonal Ekman b.ls exist, namely

$$\delta_{zonal,\,m} = (\delta_m^3 L)^{\frac{1}{4}} \ , \quad \delta_{zonal,\,s} = (\delta_s L)^{\frac{1}{2}} \ ,$$

where $\delta_m = (\nu/\beta_0)^{\frac{1}{3}}$ is the Munk b.l, $\delta_s = r/\beta_0$ is the Stommel b.l, $r = \delta_{Ek} f/(2H)$ is the linear friction coefficient, β_0 is the beta parameter, and $\delta_{Ek} = \sqrt{2\nu/f}$ is the bottom Ekman layer depth. $\beta_0 = sf/H = 0.0125\,s^{-1}cm^{-1}$ in the laboratory.

$$\Longrightarrow \boxed{\delta_{zonal,\,m} = 1.26\,cm \ , \quad \delta_{zonal,\,s} = 0.97\,cm} \ .$$

Therefore, the largest thickness of these zonal b.ls is $1.68\,cm$. If the gap width G between the cylinders is much smaller than $3\,cm$, then the viscous b.ls occupy the entire region

within each gaps, and consequently, the presence of the b.ls make the fluid within the gaps slow. This is the reason why the number of offsprings, N, decreased as G was reduced.

4 Conclusions and further studies

For $G = 3\,cm$, a dipole was observed to form in most experiments for all the configurations of the islands, however the formation of two or more dipoles never occurred. This result invalidates our hypothesis. After a dipole formed, the cyclonic part of the dipole became dominant. Depending on the configurations of the obstacles and the initial vortex position, a relatively large offspring was produced either directly from the cyclonic part of the dipole, or from the "remnant" of the original vortex at the gap positioned just "South" of the gap where the dipole was formed. We also found that intense vortices experienced relatively greater amplitude loss than weak vortices, and the number of offspring, N, was 1 in general, independently of the size of the 'middle' islands. Observations of drifters in the Caribbean Sea [11] mentioned in §1.1 might be explained from our experimental results. According to [11], large energetic anticyclonic vortices were found downstream of the Lesser Antilles and translated westward while cyclonic vortices were observed primarily near boundaries in the Eastern Caribbean Sea. The weak cyclonic vortices may have been produced from the cyclonic part of a dipole formed when a NBC ring collided with the islands. It seems likely that the dominant anticyclonic offspring was formed either directly from the anticyclonic part of the dipole, or from the "remnant" of the original vortex (after the dipole formation). When G is smaller than a critical value ($G \leq 0.7\,cm$), no vortices were formed. This may suggest that for small enough island passages, no vortices are formed in the ocean due to the presence of b.ls that can slow the fluid within the gaps. This hypotheses is hard to prove because the oceanic kinematic viscosity ν is not known for this particular process.

In the present study, the vortices were cyclonic and barotropic. Moreover, they approached perpendicularly to the chain of obstacles. On the contrary, in the ocean, NBC rings are anticyclonic and baroclinic, and they move along an oblique direction to the line of the islands. It would be interesting to see how the results described above would be modified by the inclusions of these details (i.e. anticyclonic vortices, baroclinicity, direction of propagation) in the laboratory experiments.

Acknowledgements: I would like to thank C. Cenedese for a number of useful discussions and supports, and K. Bradley for preparation the experimental apparatus. This work was completed during the Geophysical Fluid Dynamics Summer School 2005 Program at the Woods Hole Oceanographic Institution.

References

[1] Adduce, C. & Cenedese, C. (2004) An experimental study of a monopolar vortex colliding with topography of varying geometry in a rotating fluid. J. Marine Res. **62**, 611-638.

[2] Cenedese, C. & Fratantoni, D. M. & Adduce, C. (2005) Laboratory experiments on mesoscale vortices interacting with two islands. J. Geophys. Res. Vol **110**. In press.

[3] Cenedese, C. (2002) Laboratory experiments on mesoscale vortices colliding with a seamount. J. Geophys. Res. **107**, (C6).

[4] Cushman-Roisin, B. (1994) *Introduction to geophysical fluid dynamics*. Prentice Hall, Englewood Cliffs, New Jersey 07632.

[5] Fratantoni, D. M. & Glickson, D. A. (2002) North Brazil Current rings generation and evolution observed with SeaWiFS. J. Phys. Oceanogr. **32**, 1058-1074.

[6] Fratantoni, D. M. & Richardson, P. L. (2005) The evolution and demize of North Brazil Current rings. J. Phys. Oceanogr. Submitted.

[7] Jones, W. E. & Lee, T. N. & Schott, F. A. & Zantopp, R. J. & Evans, R. H. (1990) The North Brazil Current retroflection: Seasonal structure and eddy variability. J. Geophys. Res. **95**, 22103-22120.

[8] Kloosterzil, R. C. & van Heijst, G. J. F. (1991) An experimental study of unstable barotropic vortices in a rotating fluid. J. Fluid Mech. **223**, 1-24.

[9] Linden, P. F. & Boubnov, B. M. & Dalziel, S. B. (1995) Source-sink turbulence in a rotating stratified fluid. J. Fluid Mech. **298**, 81-112.

[10] McWilliams, J. C. (1984) The emergence of isolated coherent vortices in turbulent flow. J. Fluid Mech. **146**, 21-43.

[11] Richardson, P. L. (2004) Caribbean Current and eddies as observed by surface drifters. Deep-Sea Res II. **52**, 429-463.

[12] Schmitz, W. J. (1996) On the world ocean circulation. **1**, Some global features North Atlantic Circulation. WHOI technical report, WHOI-96-03, June.

[13] Simmons, H. L. & Nof, D. (2002) The squeezing of eddies through gaps. J. Phys. Oceanogr. **32**, 314-335.

[14] Whitehead, J. A. & Stern, M. E. & Flierl, G. R. & Klinger, B. A. (1990) Experimental observations of baroclinic eddies on a sloping bottom. J. Geophys. Res. **95**, 9585-9610.